Chapter 5

Measured results

Results for the SRMT designed with IE3D and Sonnet Lite and applied to actual patch antennas are presented in this chapter. It is shown that the impedance bandwidth of a patch antenna can easily be doubled when the LC-resonance is added to the feed line. Full-wave simulation comparison between the proposed matching circuit and already published techniques and structures is also presented.

5.1 Example 1: 5 mm air gap patch antenna

In Chapter 3 a patch antenna is presented in Figure 3.7 with its input impedance presented in Figure 3.8. This antenna was built as the first patch antenna example. This same antenna is now further analysed in this section. For convenience the cross-sectional geometry of the antenna is reproduced in Figure 5.1.

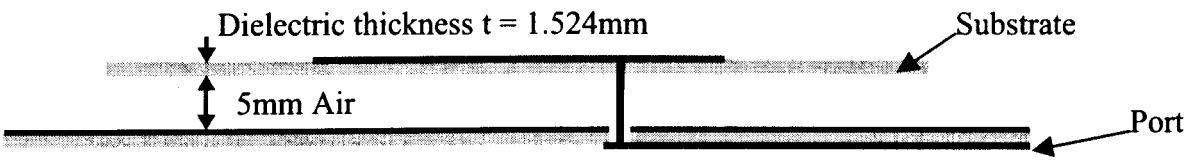

Figure 5.1 Cross-sectional geometry of the primary example patch antenna. The antenna dielectric substrate used has properties $\varepsilon_r = 3.05$ and $tan\delta = 0.003$

The dielectric substrate used for the patch antenna is GML-1000 [38] and for the feed network MC3D [39]. The dimensions of the patch antenna are W = 63 mm, L = 65.6 mm and d = 15.85 mm. The various dimensions are explained in Figure 3.1(a). The simulated and measured return loss is compared in Figure 5.2. There is good correlation between the simulated and measured results.

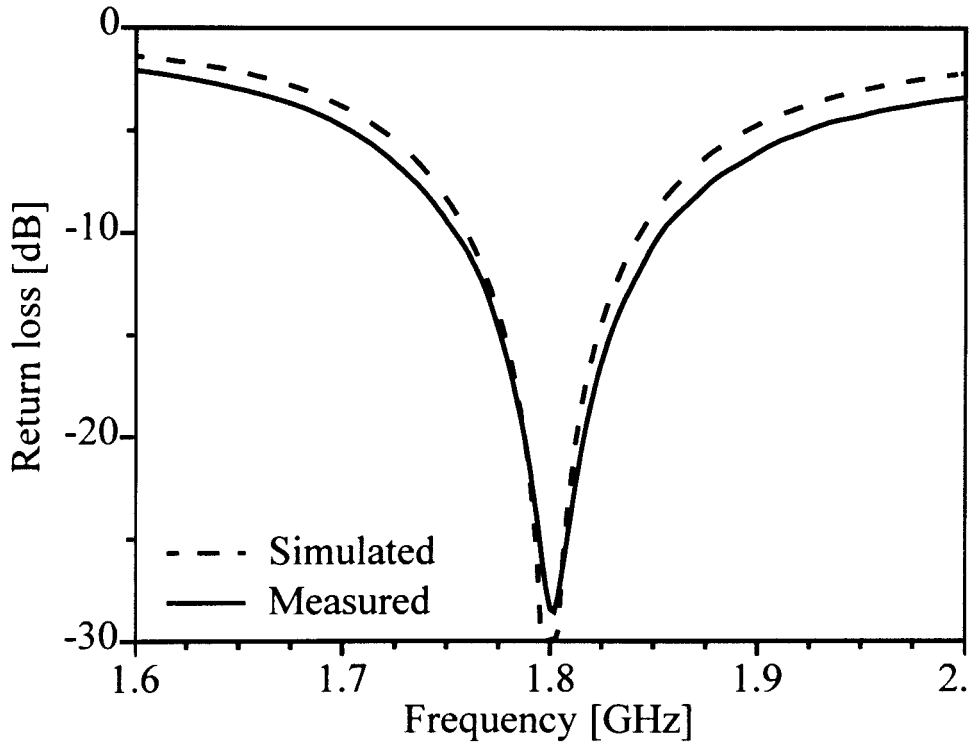

Figure 5.2 Unmatched return loss data for the 5 mm air gap patch antenna

The patch antenna is the same example as was used for the theory in Chapter 3. The various elements and transmission lines used for the SRMT on this patch have therefore already been calculated in Chapter 3. The capacitor and inductor are implemented as microstrip stubs. The capacitor is constructed as an open–ended parallel stub and the inductor is a short-circuited parallel stub. The starting values for the parallel-stub combination are obtained with equations (16) and (17).

$$Z_{OL} \tan(\beta l) = X_{HL} \qquad \text{(inductive)} \qquad (16)$$

$$\frac{Z_{OL}}{\tan(\beta l)} = X_{HC} \qquad \text{(capacitive)} \qquad (17)$$

The patch antenna example was designed to obtain optimum VSWR < 1.5:1 bandwidth. The required components for the matching circuit consist of (refer to Table 3.1) a 50 Ω transmission line of 37°, a parallel LC-section with element values of 0.768 nH and 10.45 pF, and a quarterwave transformer with $Z_{\lambda/4}$ = 61.2 Ω.

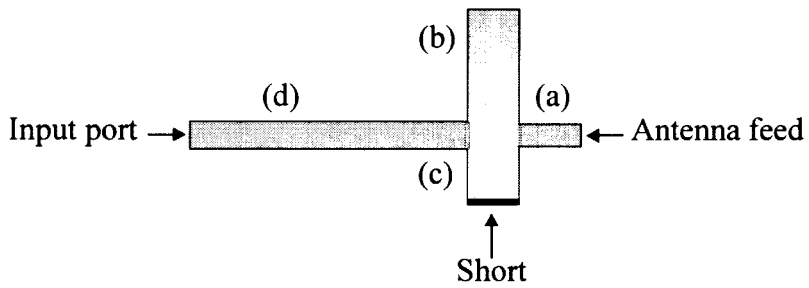

Figure 5.3 Circuit layout for the SRMT. The components are placed in the following order: (a) phase transformer, (b) and (c) capacitor and inductor respectively, and (d) quarterwave transformer

A number of problems were encountered when the circuit shown in Figure 5.3 was first simulated. The main issue was uncertainty regarding the reference position of the stubs. The exact location where the phase transforming transmission line and the quarterwave matching circuit should start and end was not accurately known when starting with the theoretically calculated values for all the elements in the circuit. With these unknown parameters in mind it was decided to do the conversion from theoretical component values to microstrip line step by step. These steps are explained in the next paragraphs.

The first step in the design is to ensure that the phase transforming circuit is correct. The desired transformation is a known parameter, and with the aid of this information the microstrip version of this transmission line can be optimised. In IE3D the transmission line

was combined with the patch antenna shown in Figure 5.1. The 50 Ω line is then tweaked to exactly the right length so that the phase transformation is correct.

The resonance and placement of the capacitor and the inductor are the next step. The distributed LC-section is first optimised to obtain the correct resonance, after which the placement with respect to the phase-transforming transmission line is considered. If all the elements are placed close to a third of the tangential line width inwards, good starting values were obtained. Figure 5.4 illustrates the position of this "one third".

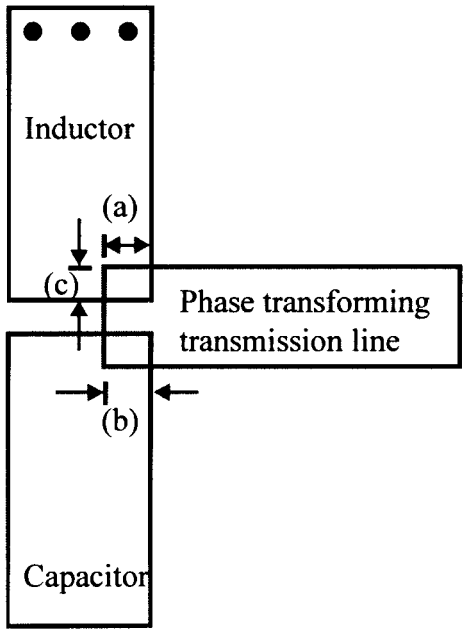

Figure 5.4 Illustration to show where the distributed components are placed before final optimisation. Positions (a) and (b) show how the phase transformation line is placed one third of the elements' width into the junction, and (c) shows how the distributed elements are placed one third of the transmission width inwards from the edge

The positions described here are not based on any previously published research. It is simply a starting value from where the capacitive and inductive stub lengths and positions are tweaked further.

Lastly the quarterwave transformer is added to the circuit. The transformer is normally close to correct without too much tweaking.

An important issue encountered is the pronounced effect of the probe connecting the microstrip feed network to the antenna port, situated on the ground plane (see Figure 5.5 for a graphical representation).

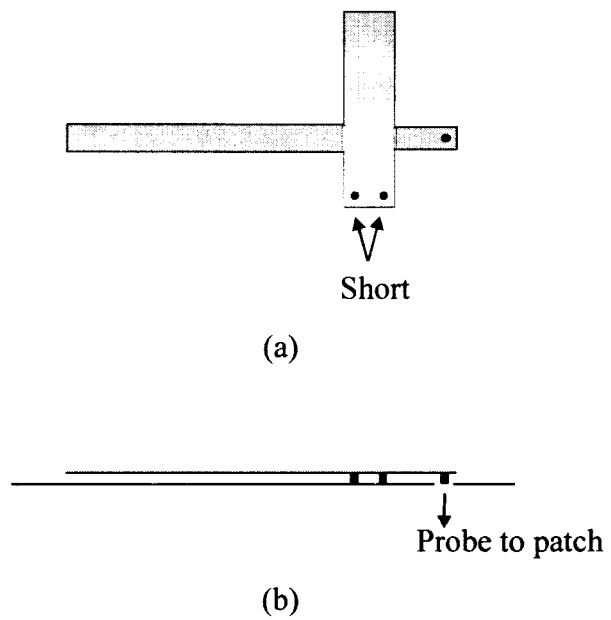

Figure 5.5 Top view of the fully modelled microstrip feed line (a) and a side view to illustrate the position and layout of the shorting pin and feed probe (b)

The connection line between the patch antenna feed probe and the microstrip line is important to include in the design. The importance of the connection line lies in the fact that it is effectively a small piece of transmission line. This piece of line does not exhibit the required characteristic impedance of 50Ω and contributes to the phase and impedance transformation of the input impedance. Compensation for this component can be done by simply including the probe (as shown in Figure 5.5) in the network design from the start. The inclusion is very simple to do in IE3D, and results in the length and width of the phase transforming transmission line changing slightly from the initially predicted dimensions.

The reason for using two shorting vias (as opposed to one) in the inductor stub (Figure 5.5) is that the stub width is fairly large compared to the shorting via. The ideal case would be to have a shorting plane at the end of the stub.

For all the probe-fed antenna examples presented in this dissertation, an evaluation of the resonant section of the matching circuit is included. This was done in order to verify that it is possible to implement the parallel-LC circuit section with the proposed open and shorted stubs. Figure 5.6 presents the imaginary admittance response obtained with the parallel capacitor and inductor required for the 5 mm air gap patch antenna.

Figure 5.6 illustrates how one can closely obtain the ideal resonant response for the matching circuit with distributed components. The most important factor in the resonant design is the straight-line frequency response, since this is the essence of the SRMT. As described earlier in this section, it is good to consider the phase transforming transmission line alone at first. Also, as shown in Figure 5.6, it is good to get the resonance close to the correct level in terms of resonant frequency and imaginary admittance values. One must, however, keep in mind that the most important result is the final return loss for the antenna integrated with the feed network. Therefore it is important to get the individual components close to the correct values, as in Figure 5.6. Once the individual components are satisfactory it is more important to combine the system and tweak the components for optimum overall results. A guideline for satisfactory results for the resonant section is that the centre frequency should be at least within 10% accurate, and the imaginary admittance values at the design frequency should also be within this margin. This guideline is applicable to the 5 mm air gap patch antenna, and will also work for wider bandwidth patch antennas. The second example of this chapter is an extremely narrow band patch antenna (1% bandwidth), and in that case much more care must be taken to obtain accurate results. More will be said about this in the next section.

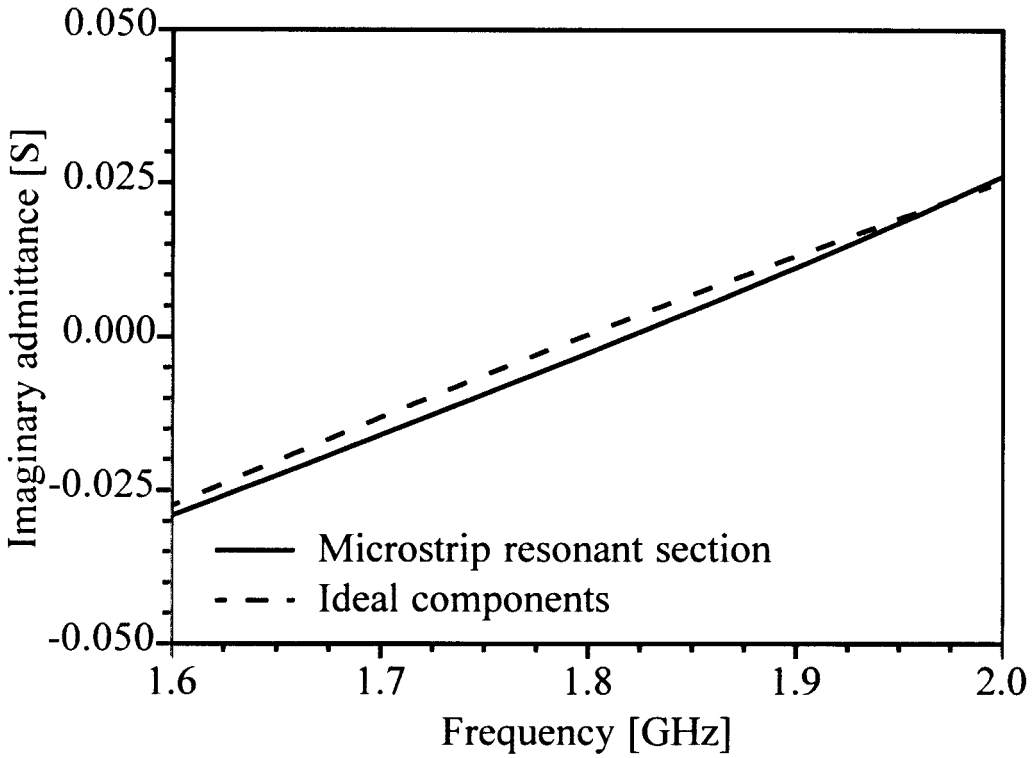

Figure 5.6 Comparison obtained in initial design between the theoretical parallel-LC section, and the implemented open- and short-circuited stubs. Both are for the 5 mm air gap patch antenna

The simulated results for the patch antenna with and without the matching circuit are shown in Figure 5.7. The response shown is for the final simulated circuit, in other words no additional tweaking is required for this circuit anymore. The design VSWR specification is 1.5:1. In Figure 5.7 one can see that the aim is not to be too close to maximum return loss value, since manufacturing tolerances should be kept in mind.

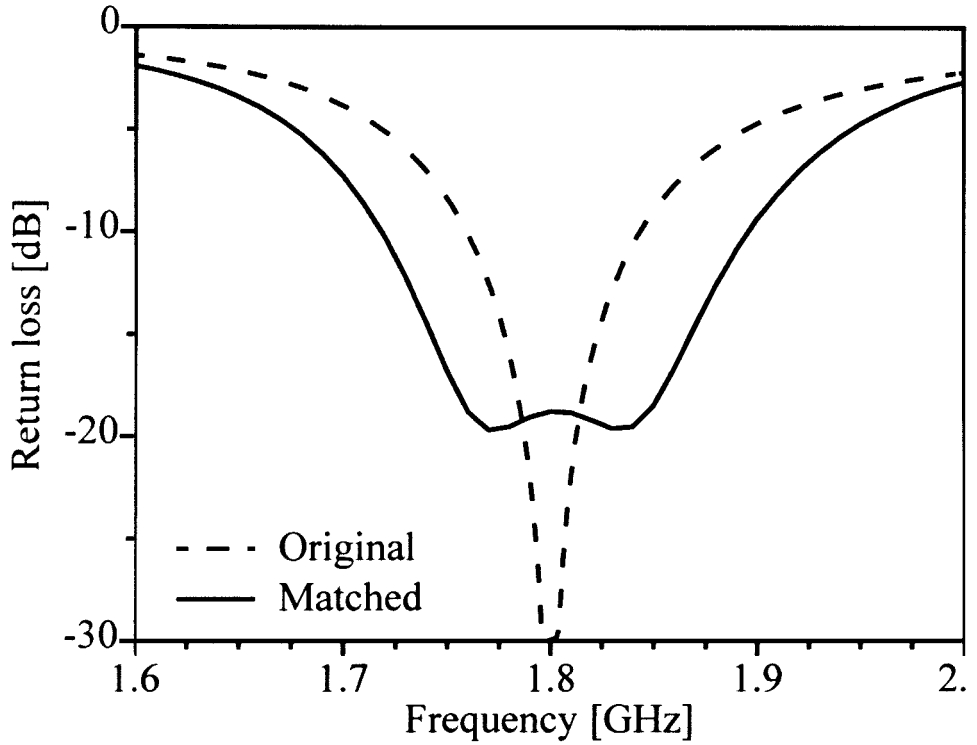

Figure 5.7 Simulated results for the patch antenna with the inclusion of the matching network for bandwidth improvement

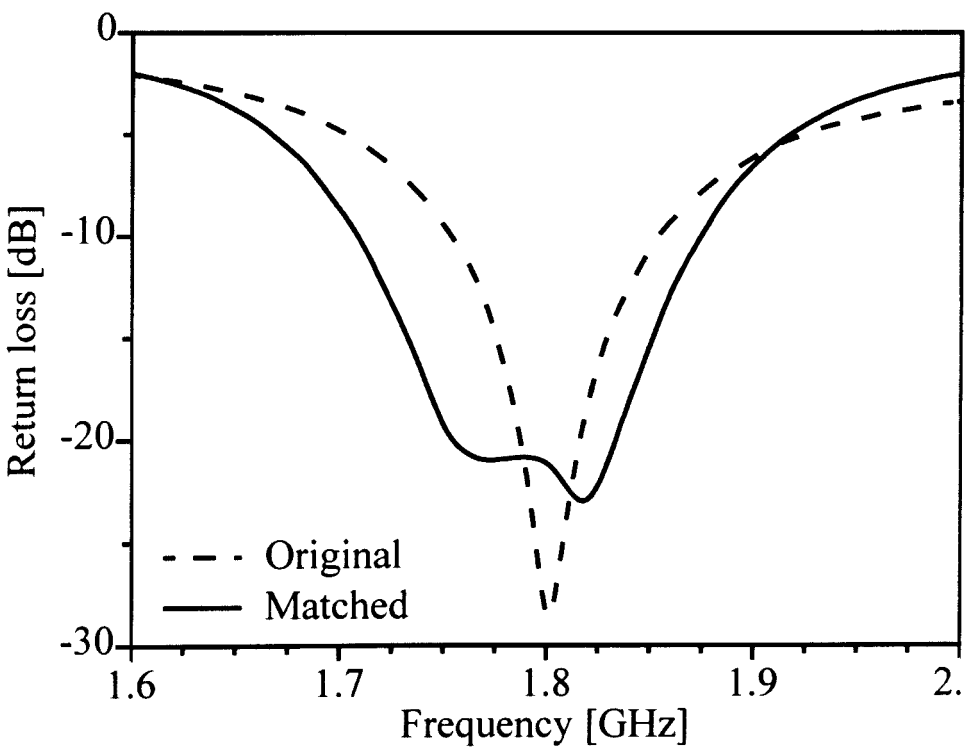

Figure 5.8 Measured results for the matching network when applied to the patch antenna example

The original simulated antenna in Figure 5.7 has a bandwidth of 50 MHz, between 1.78 and 1.83 GHz. The addition of the SRMT matching section resulted in an improved bandwidth of 130 MHz, from 1.74 GHz to 1.87 GHz.

Figure 5.8 shows the measured return loss for the antenna. The measured bandwidth of the antenna without the matching network was 59 MHz, from 1.773 to 1.832 GHz. This compares very well with the predicted values obtained by IE3D. The impedance matched antenna had a VSWR < 1.5:1 between 1.728 and 1.855 GHz, presenting a 127 MHz bandwidth, again corresponding very closely with the simulated result.

In the measured result a slight asymmetry can be observed in the return loss plot shown in Figure 5.8. This is due to a minor reactive component in the input impedance, most probably caused by assembly inaccuracies. On the Smith chart one would be able to notice that the "eye" is not perfectly placed around the centre of the chart, but moved slightly upward or downward. If this becomes a problem, it can be resolved by tweaking either the capacitor or the inductor used in the LC-match. The match itself increased the VSWR bandwidth from 59 MHz to 127 MHz. This is an increase of 68 MHz, or 115%. Table 5.1, included at the end of the chapter, summarises all the results presented in this chapter, expressing the results both in terms of frequency bandwidth and percentage improvement.

The impedance bandwidth of the patch antenna increased to more than double the original value. This is very promising, but in order to be able to characterise the improved patch antenna, the radiation patterns are also considered. The patterns are calculated using IE3D and compared to the patterns measured for the patch antenna with and without the matching circuit. The normalised E-plane patterns for 1.8 GHz are presented in Figure 5.9. The H-plane co-pol patterns are shown in Figure 5.10 and the cross-pol patterns in Figure 5.11, both at 1.8 GHz.

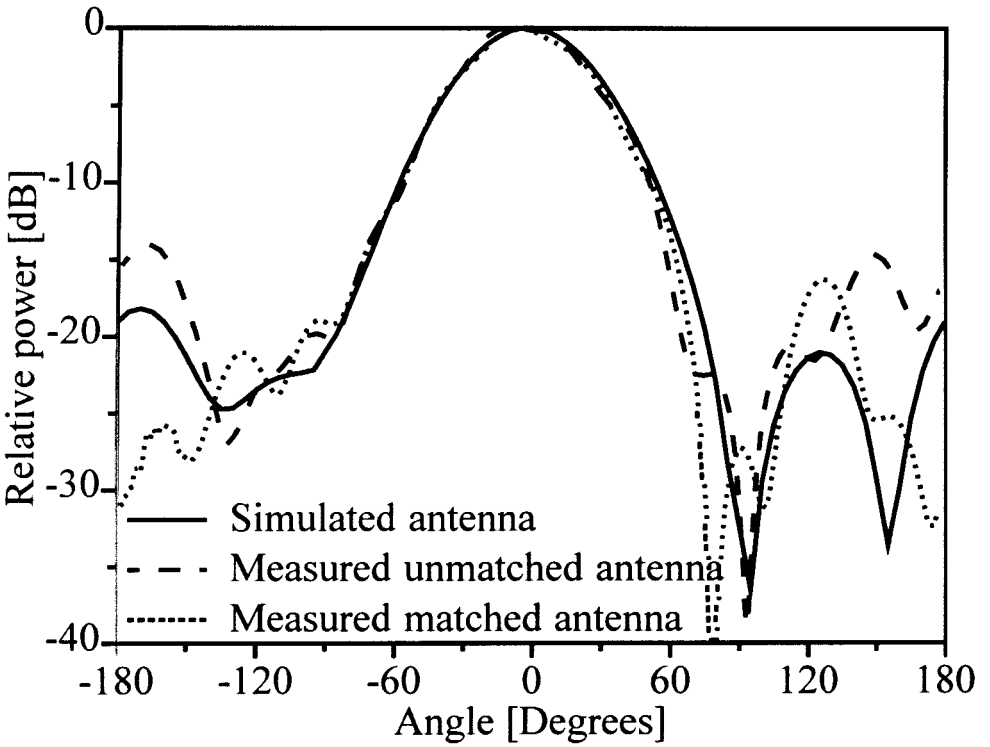

Figure 5.9 E-plane radiation patterns (1.8 GHz) of the patch antenna, comparing the results obtained for the simulated patch against the two measured unmatched and matched antennas. The simulated antenna is considered without a feed network, only a finite ground plane

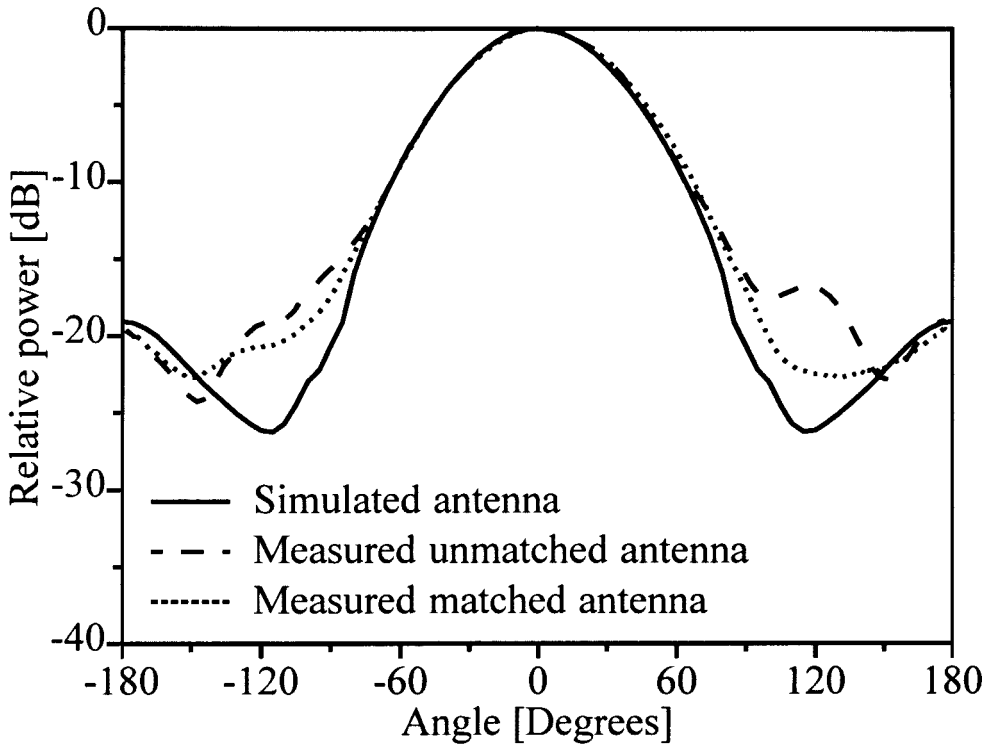

Figure 5.10 H-plane co-pol radiation pattern for the different types of antennas at 1.8 GHz

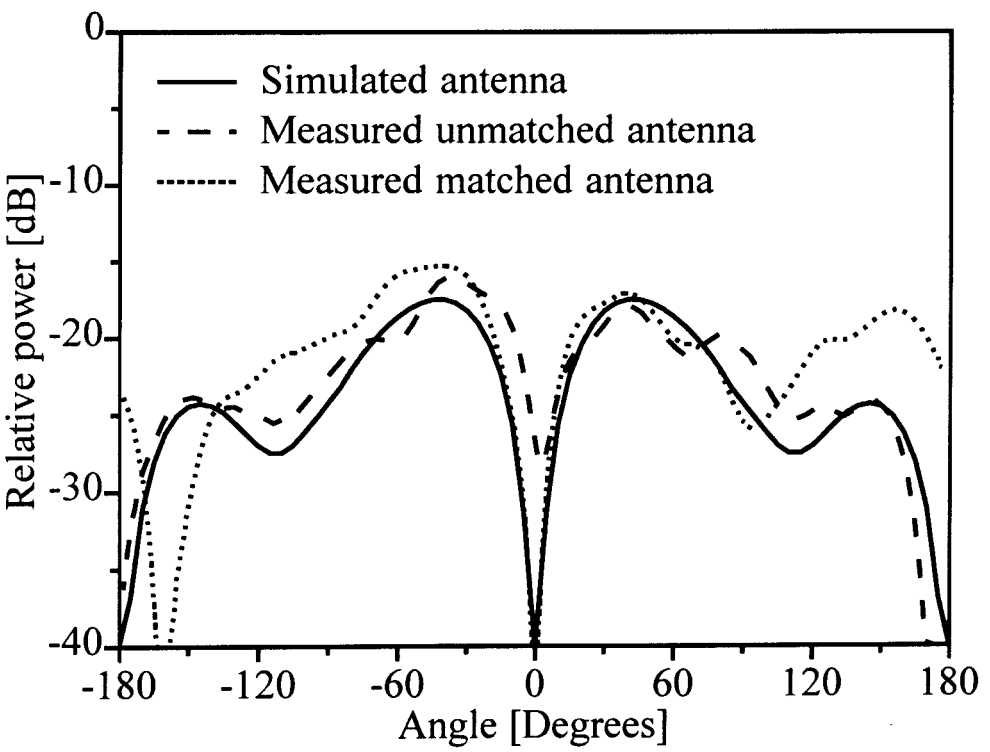

Figure 5.11 H-plane cross-pol radiation pattern for the three antennas considered, all at 1.8 GHz

It is evident that the radiation pattern obtained using the simulation software is, as was the case for the return loss results, very close to the measured results. In all three figures one can clearly see that the difference obtained is very small, and most often the main differences are encountered at levels of 15 dB or more down from the peak value. The possibility that unwanted radiation is encountered as a result of the addition of the open- and shorted stub is unlikely, and Figure 5.9 to Figure 5.11 shows this clearly. The only real noticeable deviation is visible in the H-plane cross-pol pattern, although the levels still remain nominally below –15 dB. The main lobe remains virtually unchanged when compared in the three antennas. This proves that the uncertainty in respect of the differences in the back lobe regions might be part of the feed network, as well as radiation obtained from the edges of the ground plane and construction errors.

Patch antennas in general have a relatively wide radiation pattern bandwidth [3]. The bandwidth operation is most often limited by the specified return loss bandwidth. In order to evaluate the radiation pattern as a function of frequency for the matched patch antenna, three radiation pattern graphs are presented in Figures 5.12 to 5.14. Only the graphs of the measured SRMT-matched antenna are included. Three different frequencies are shown, namely 1.74, 1.8 and 1.86 GHz.

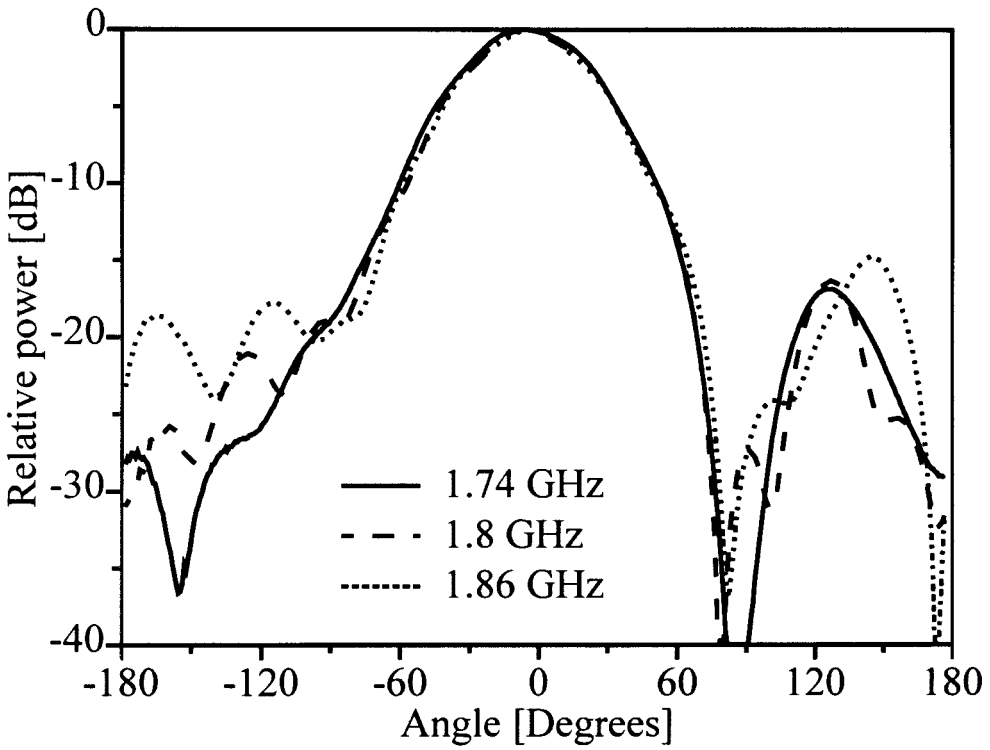

Figure 5.12 Measured E-plane radiation pattern of the SRMT-matched patch antenna at three operating frequencies

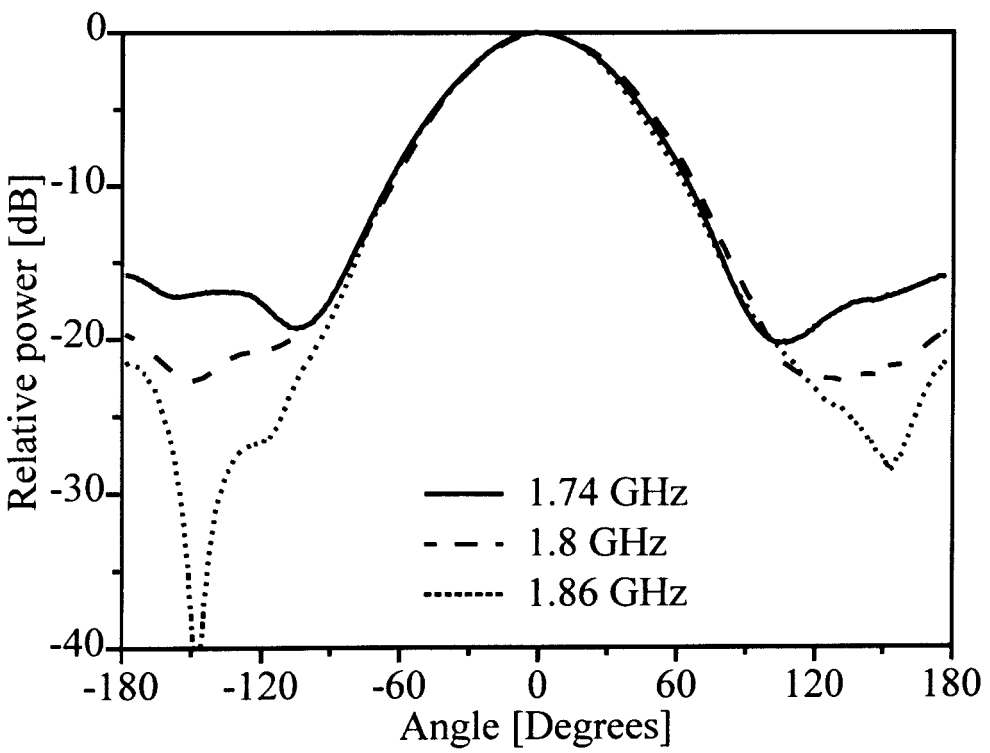

Figure 5.13 Measured H-plane co-pol radiation pattern of the patch antenna

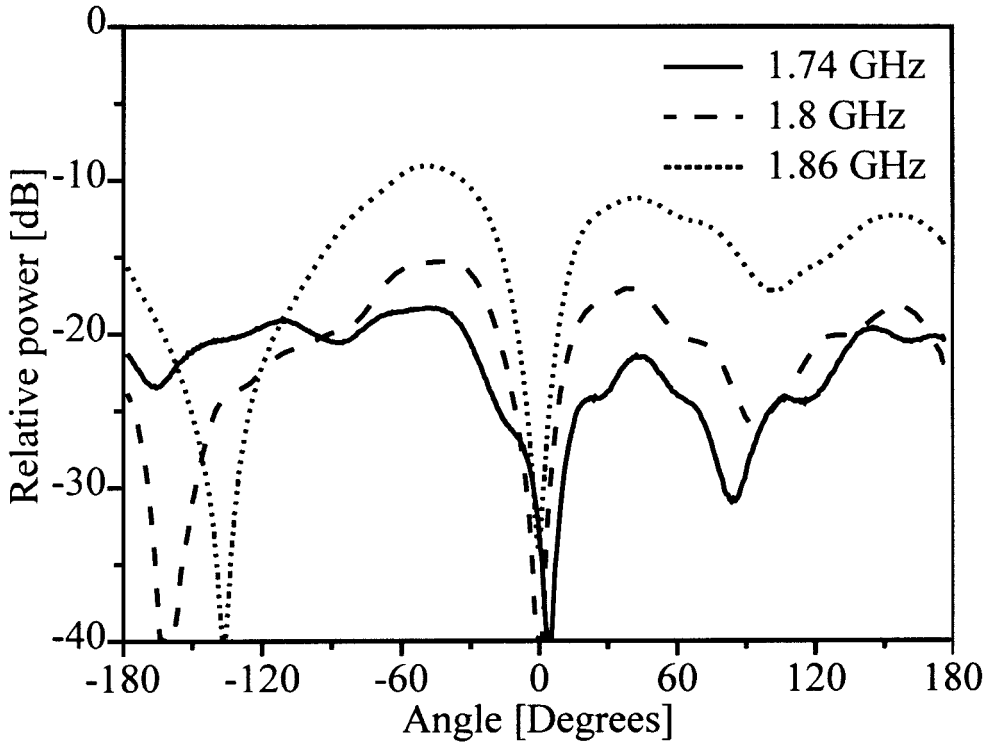

Figure 5.14 Measured H-plane cross-pol radiation pattern of the antenna

The main beam co-pol patterns for the different frequencies in both the E- and H-plane are relatively constant over the frequency range considered. In both Figures 5.12 and 5.13 the beam remains the same for the range ±90°, with minor differences visible at the edges very close to 90°. The variation that is visible in the E-plane pattern shown in Figure 5.12 in the vicinity of –90°, is the location where the connector was placed. Therefore the slight variation in pattern may be attributed to scattering from the connector interface, as well as the cable position during the measurement setup. The measured H-plane cross-polarisation measured for the patch antenna seems somewhat untidy. Some of the problems encountered can be attributed to construction errors and scattering from the finite ground plane edges as well as the connector and feed cable. Despite all this, the H-plane cross-polarisation has the standard shape that is associated with it, namely a null in the 0° direction, as well as maximum levels in the region of ±45° to ±60°. Also clear is the fact that the maximum value increases as the frequency increases. To correlate this with theory, the simulated cross-polarisation patterns are shown in Figure 5.15.

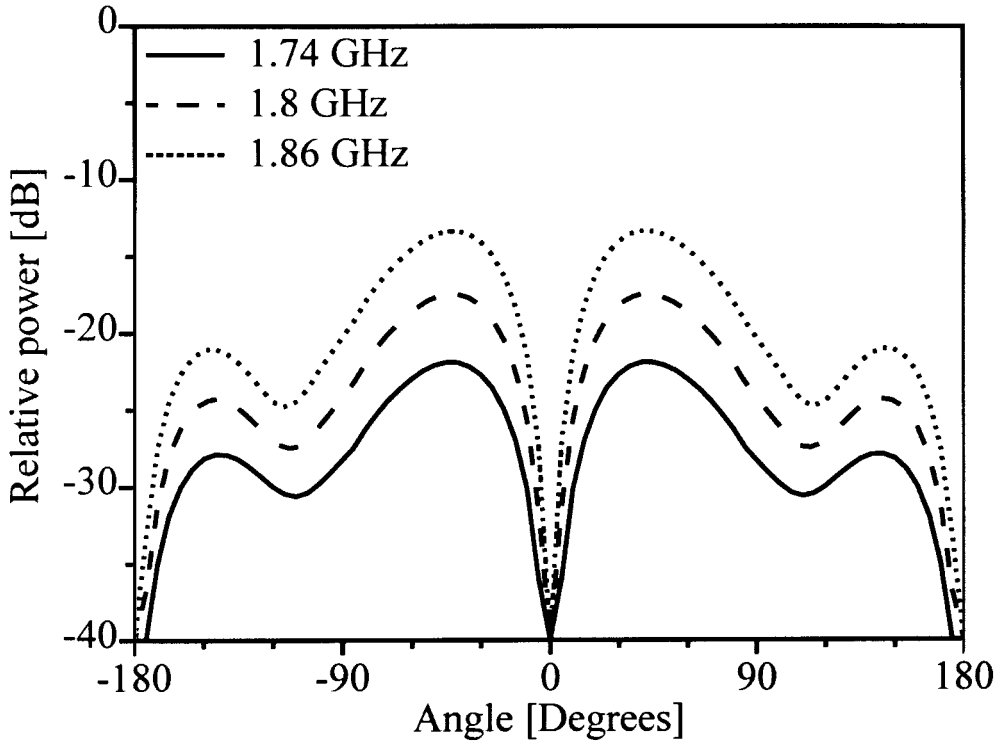

Figure 5.15 Simulated H-plane cross-polarisation with a finite ground plane

Despite the slight asymmetry of the radiation patterns in Figure 5.14, the resemblance between the simulated data in Figure 5.15 and the measured data is still visible and quite acceptable. The overall results prove that the addition of the matching network had a negligible effect on the radiation properties of the patch antenna.

Figure 5.16 presents the measured gain for the unmatched and matched patch antennas. The gain was measured between 1.7 and 1.9 GHz since this was mainly the frequency range of interest. According to the IEEE Standards (Page 59 in [36]): "gain does not include losses arising from impedance mismatches and polarisation mismatches". Therefore the term 'gain' used in this dissertation should strictly be considered measured gain with reference to the standard gain antenna (the measured gain presented here does include mismatch losses) and not the IEEE Standards definition of gain.

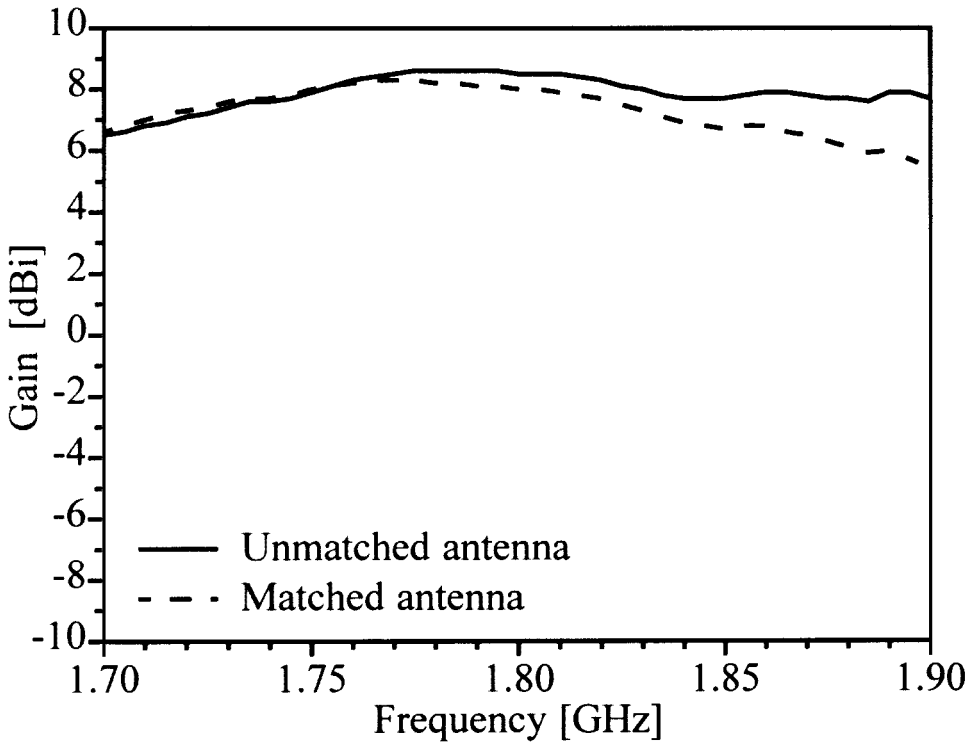

Figure 5.16 Measured gain response for the 5 mm air substrate antenna

An important note on this result is the fact that is seems as if the gain drops slightly for the antenna to which the SRMT-circuit was added. The maximum gain value measured for the patch without the SRMT-circuit is 8.6 dBi, and for the antenna with the LC-section added a maximum gain of 8.3 dBi was measured. The main difference is the fact that the gain peak for the matched antenna is at a lower frequency than the patch antenna without the SRMT circuit. In Figure 5.8 the slight frequency shift between the matched and unmatched antenna is illustrated. It is reasoned that this is mainly due to the additional losses added by the SRMT-circuit, and to a lesser extend the fact that the resonance of the actual load (the patch antenna) and the resonance of the LC-circuit are slightly displaced in frequency from one another. The combined resonance results in a final intermediate resonance with slightly compromised gain.

5.2 Example 2: Narrow band patch antenna

The outline of the second example patch antenna built is shown in Figure 5.17. The antenna is made with dielectric substrate only, and no air gaps are included. It is referred to as the "substrate-only" patch antenna. The dielectric substrate used for both the patch antenna and the feed network is GML-1000 [38].

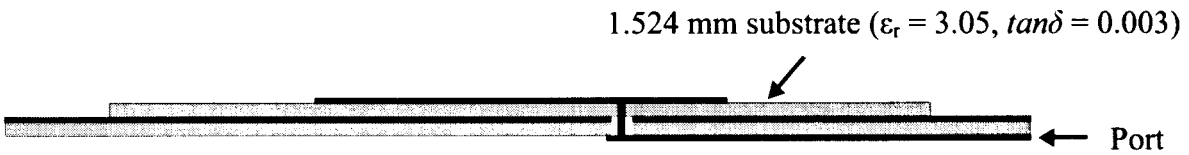

Figure 5.17 Outline of the "substrate-only" patch antenna

The design parameters for the patch antenna to have a minimum return loss at a centre frequency of 1.8 GHz are as follows (all dimensions in millimeters): d = 14.15, W = 60 and L = 46.3. The patch was designed and simulated in IE3D, after which it was built as shown in Figure 5.17. The simulated and measured results are shown in Figure 5.18.

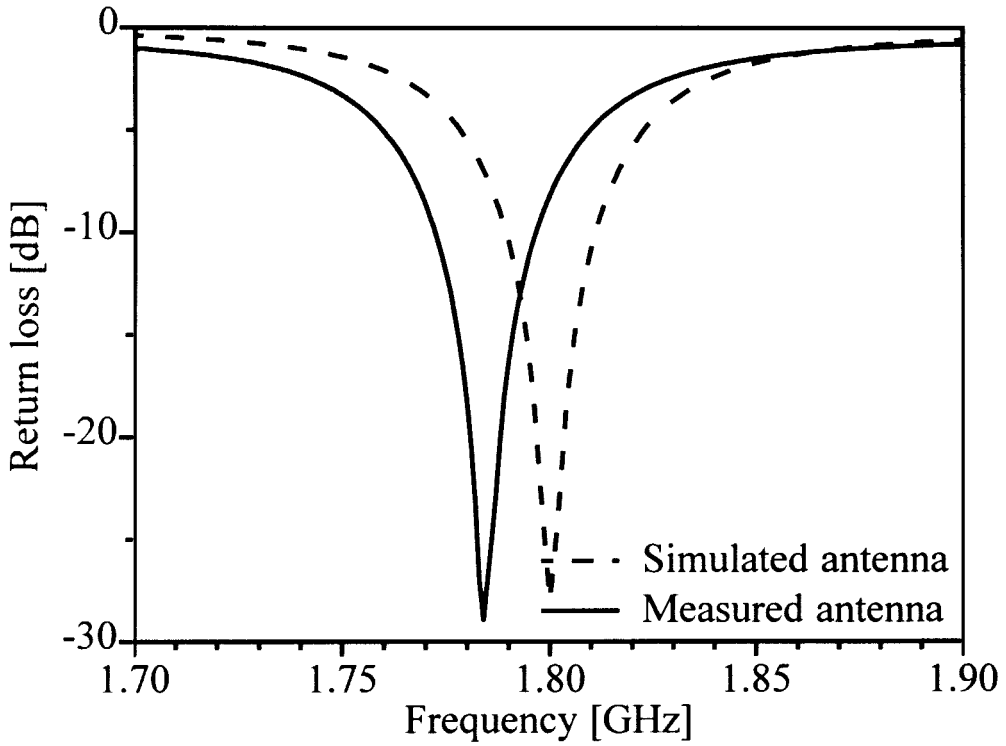

Figure 5.18 Measured and simulated return loss of the "substrate-only" patch antenna

In Figure 5.18 a frequency shift between the simulated prediction and the actual patch antenna is evident. The frequency shift obtained is 1%, and the VSWR bandwidth (1.5:1) of the patch antenna is also in the order of 1%. The "substrate-only" patch antenna is extremely sensitive to any type of variation in either the construction or the properties of the dielectric substrate. Although this 1% deviation might pose a problem in practice, the aim with this patch antenna is to prove an experiment and not so much to design a nearly perfect antenna. Therefore it was decided to keep the patch antenna as it is, and rather design a matching network that will work for the patch antenna example considered. The resonant frequency of the patch antenna is now 1.785 GHz. The design of the patch antenna's matching network was based on the measured data. In illustration, the theoretical predictions are included for the original simulation, and the full wave simulation as well as the measured matching results for the physical patch antenna.

The simulated "substrate-only" patch antenna, with and without the theoretical matching network, is presented in Figure 5.19. The matched specification is considered for a VSWR < 1.5:1. The original (unmatched) antenna has a bandwidth of 14 MHz (1.793 – 1.807 MHz), and the inclusion of the theoretical matching network improved the bandwidth to 33 MHz (1.784 – 1.817 MHz).

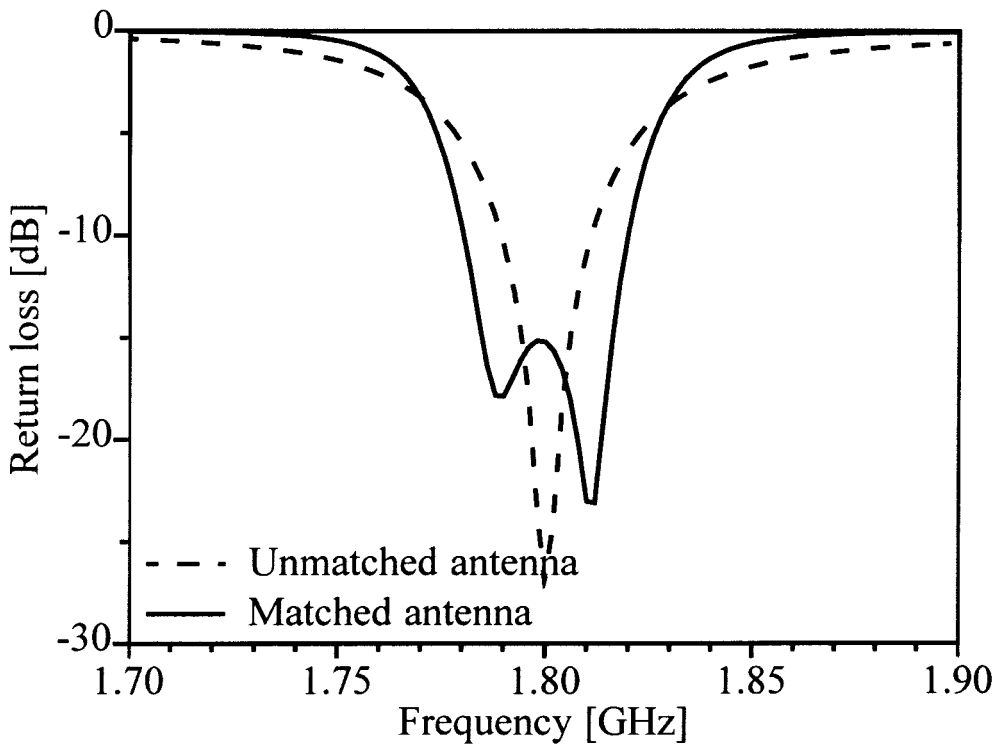

Figure 5.19 Theoretical bandwidth improvement of the "substrate-only" patch antenna

The measured antenna's input impedance has been used for the design of the actual matching network. Despite the slight frequency shift of 1% the component values are very close to those obtained for the theoretical design. The phase-transforming transmission line is 77.5° and the quarterwave matching line impedance 58 Ω. The capacitor used in the matching circuit is 27.807 pF and the inductor 0.286 nH.

In the previous section it was stated that the admittance response can be considered satisfactory in the initial design once the centre frequency and the admittance levels are within a 10% margin. For the "substrate-only" patch antenna this is not good enough. It

was found the final result must be extremely close to the required levels. For the theoretical values of the capacitor and the inductor, variation on the third decimal made a difference to the final result. For the microstrip simulation done in IE3D and Sonnet Lite a change in stub length in the order of 0.05 mm resulted in considerable variation in the final return loss. With this in mind, it must also be said that the measurement results presented in this section required a lot of patience to find the exact length of the stubs.

Figure 5.20 presents the final simulated resonant admittance curve for the above-mentioned LC-section as well as the microstrip resonant section for the "substrate-only" patch antenna example.

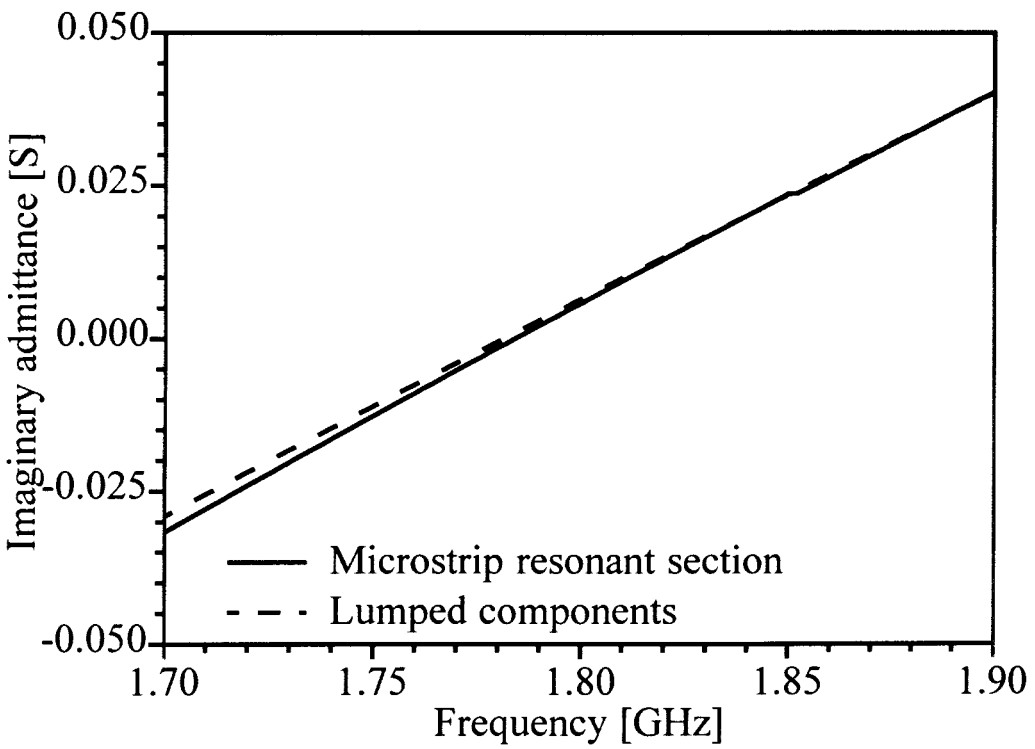

Figure 5.20 Theoretical and microstrip equivalent admittance response for the parallel-LC combination required for the "substrate-only" patch antenna

Figure 5.20 illustrates how the open- and shorted stubs implemented as equivalent circuit elements can result in very accurate circuit components. One phenomenon that is not evident from Figure 5.20, but was observed during the study, is that there is always a remarkable improvement between the theoretical predictions made and the final full wave

simulation and measurement. Figure 5.20 illustrates that this is probably not due to the difference in admittance response between an ideal LC-circuit and the stubs, but rather to the interfaces between the stubs and the various transmission lines.

Figure 5.21 presents the results obtained with IE3D for the matching network applied to the measured patch antenna. This was done because the measured antenna had a slight frequency shift, and by taking this frequency shift into account one will achieve a more reliable design.

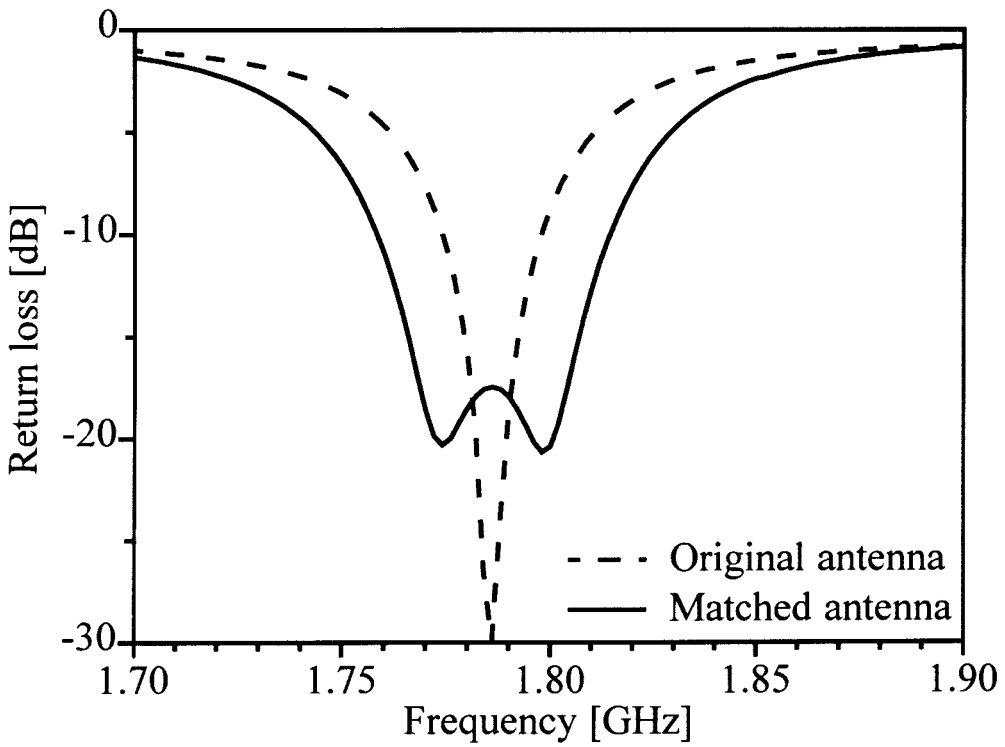

Figure 5.21 Simulated matched response, with the return loss of the measured antenna included, and also used as load for the simulation of the circuit

The simulated results for the matching network predicts a –14 dB bandwidth of 43 MHz (1.765 GHz – 1.808 GHz). The original antenna bandwidth is 15 MHz. This results in an improvement close to three times the original bandwidth.

Figure 5.22 presents the measured return loss for the matching network. The original antenna considered in this figure is the same one as in Figure 5.21.

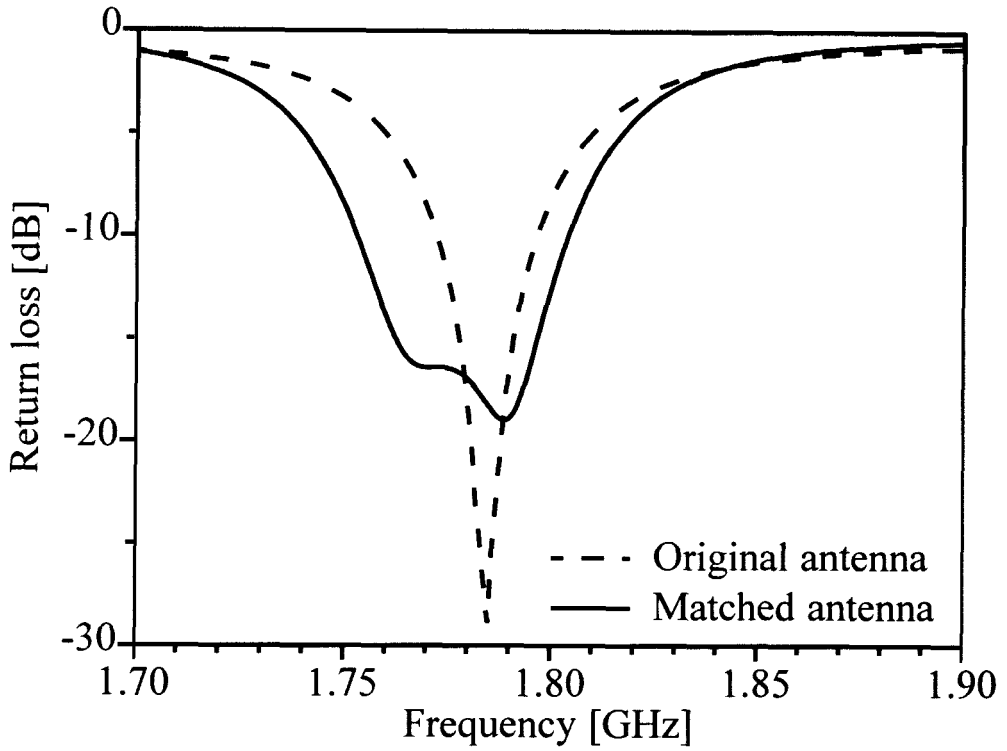

Figure 5.22 Measured bandwidth improvement of the "substrate-only" patch antenna

The measured improvement with the inclusion of the SRMT matching network is 37 MHz (1.761 – 1.798 GHz). The improvement is slightly less than the predicted improvement, but the factor is still much more than double the original return loss bandwidth. A slight asymmetry can be observed in the return loss result, similar to the measured result presented in Figure 5.8. This is once again probably caused by construction errors, as well as possible inaccuracies encountered by the simulation software. Although this might be the case, the results are still acceptable since a remarkable improvement in bandwidth is observed.

The gain of the patch antenna for unmatched and matched case is presented in Figure 5.23. The gain curve presented in Figure 5.23 differs from the gain presented in Figure 5.16. The main difference is in the fact that the "substrate-only" antenna is much narrower in its operating bandwidth, and the frequency range considered is thus much wider in comparison to the antenna bandwidth.

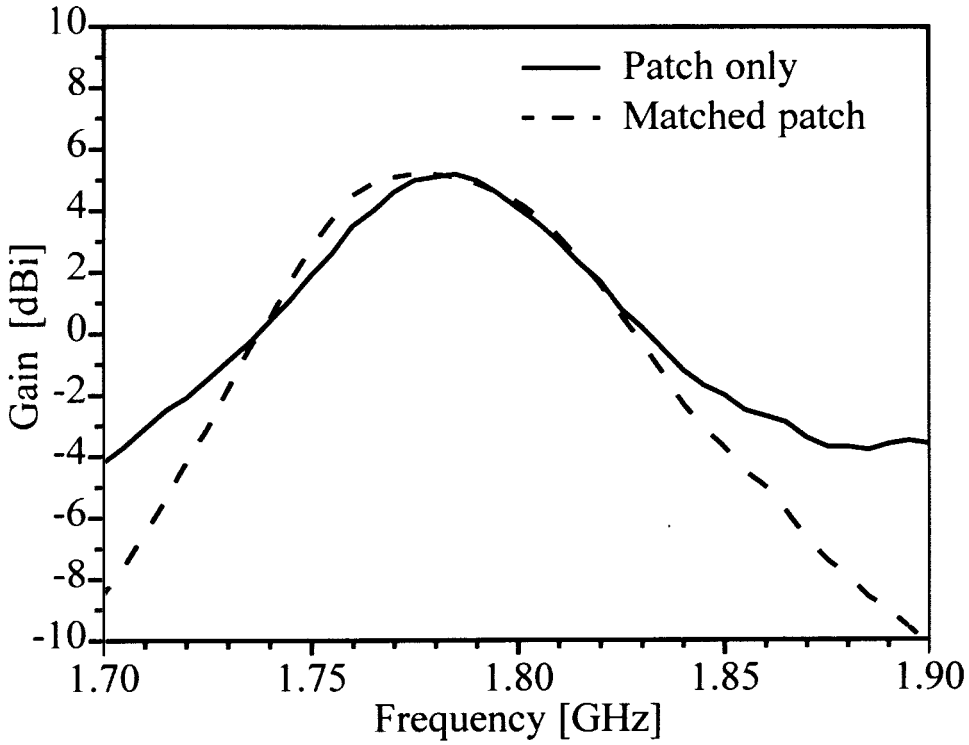

Figure 5.23 Measured gain for the "substrate-only" patch antenna

With the data shown in Figure 5.23 a number of important observations can be made, which is not evident in Figure 5.16. Note that a slight frequency shift similar to the shift obtained between the matched and unmatched antenna in Figure 5.19 is evident in the gain response. The centre frequency of the matched antenna is slightly lower than that of the unmatched antenna. The addition of the SRMT-circuit not only results in a wider return loss frequency range, but in Figure 5.23 one can see that the gain tends to remain close to the maximum value over a wider frequency range. If the frequency band is considered where the gain drops by 1 dB from the maximum, the unmatched patch antenna has a 35 MHz bandwidth around 1.785 GHz and the matched antenna 43 MHz with a centre frequency of 1.778 GHz. Both antennas have a maximum gain of 5.2 dBi. The out-of-band gain is lower when the SRMT-circuit is added. This is generally not a problem, since the antenna is not supposed to be operating at these frequencies.

5.3 Example 3: 10 mm air patch antenna

The SRMT was also applied to a patch antenna that is in itself already wideband. It is important to note that the usage of wideband in this dissertation is a relative term. When this antenna is called wideband, it is done so in comparison to the first two example patches. In itself, when compared to other wideband antennas, this example might prove rather narrowband. A patch antenna with the feed technique proposed by Mayhew-Ridgers et al. in [5] was designed for a resonant frequency of 1.8 GHz with an air gap of 10 mm between the ground plane and the supporting patch antenna substrate. The design and layout are shown in Figure 5.24. The parameters for the patch are as follows (all dimensions in millimetres): $w = 5$, $l = 24.6$, $y = 5.2$, $W = 58.2$, $L = 64$. The patch as well as the matching transmission line is etched on MC3D [39]. Please take note that the parameters for the main radiating patch are not defined in the same way as for the previous two patches, see Figure 5.24. The dimensions for this patch antenna are considered with respect to the small coupling patch that is connected to the probe.

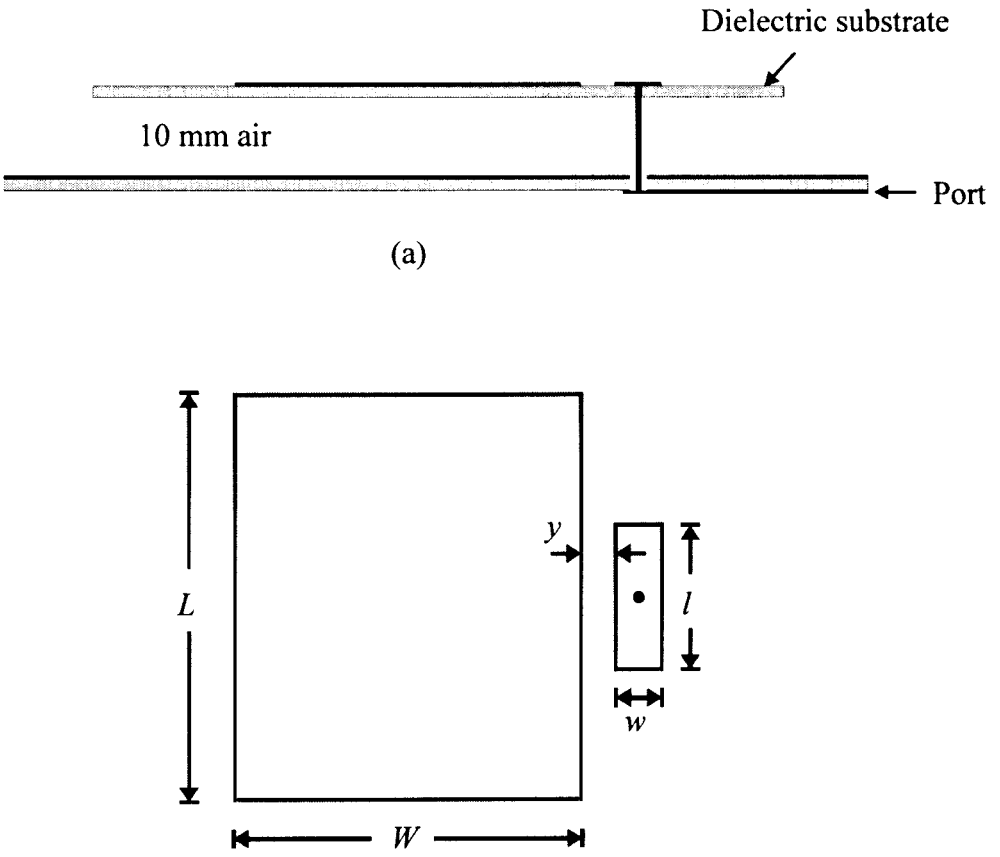

Figure 5.24 Design parameters for the capacitive-fed patch antenna with a 10 mm air gap. (a) presents the side view, and the top view with the inclusion of the parameters is given in (b)

The patch antenna was designed and simulated in IE3D. The capacitor required for the antenna is 1.77 pF and the inductor 4.4 nH. The admittance response for both the lumped components and the preliminary microstrip resonant section (i.e. before integration with the phase and impedance transforming transmission lines and the antenna itself) is shown in Figure 5.25. As was the case with both previous patch antenna examples, the resonant behaviour of the lumped LC-section can be obtained very accurately with the microstrip stubs.

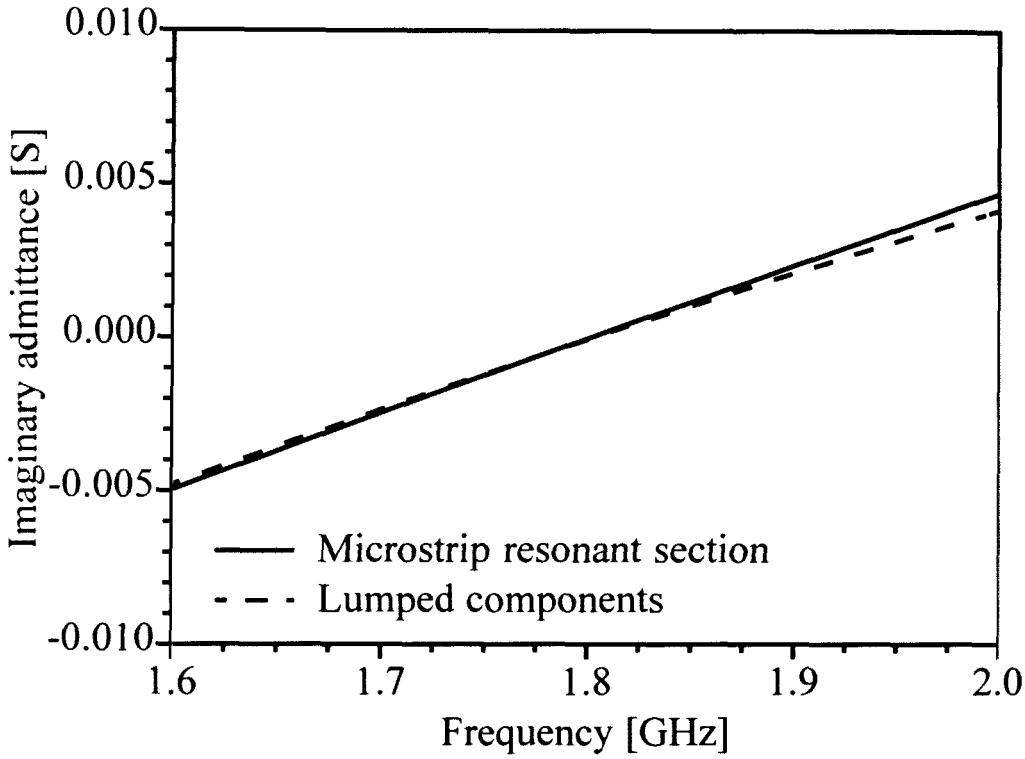

Figure 5.25 Resonant section design for the 10 mm air gap patch antenna example

The simulated return loss and the improvement with the addition of the matching circuit are shown in Figure 5.26. The original patch antenna has a VSWR < 1.5:1 frequency range between 1.723 and 1.879 GHz, presenting a 156 MHz band. The inclusion of the matching network increases the frequency band to 290 MHz (1.66 – 1.95 GHz). This is a very large frequency band, much larger than the previous two example patch antennas. The improvement obtained with the addition of the matching network is 86%, not exceeding more than double the original band. Figure 5.27 presents the measured results obtained for the antenna. A slight downward frequency shift is evident with the addition of the matching circuit. This is also evident in the previous two measured examples, implying that the occurrence might be attributed partly to the simulation software or the specific way all three the example patches were constructed. The original antenna has a VSWR < 1.5:1 bandwidth of 159 MHz, from 1.716 to 1.875 GHz. The addition of the matching network resulted in a new frequency bandwidth of 261 MHz between 1.656 and 1.917 GHz. The increase in bandwidth is 64%.

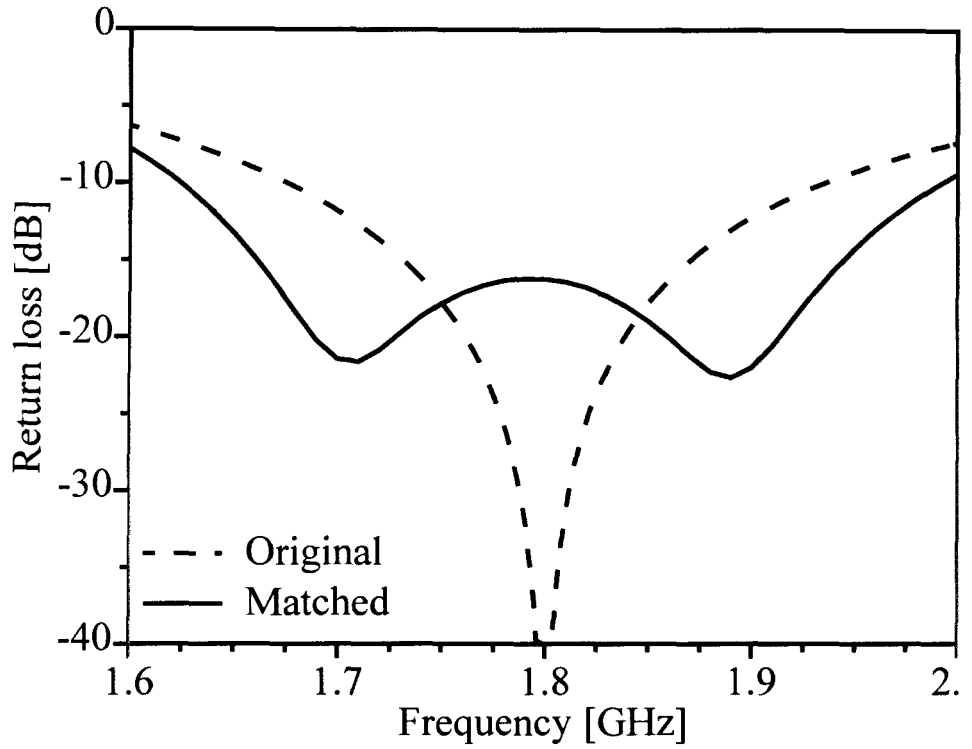

Figure 5.26 Simulated return loss for the 10 mm air patch antenna

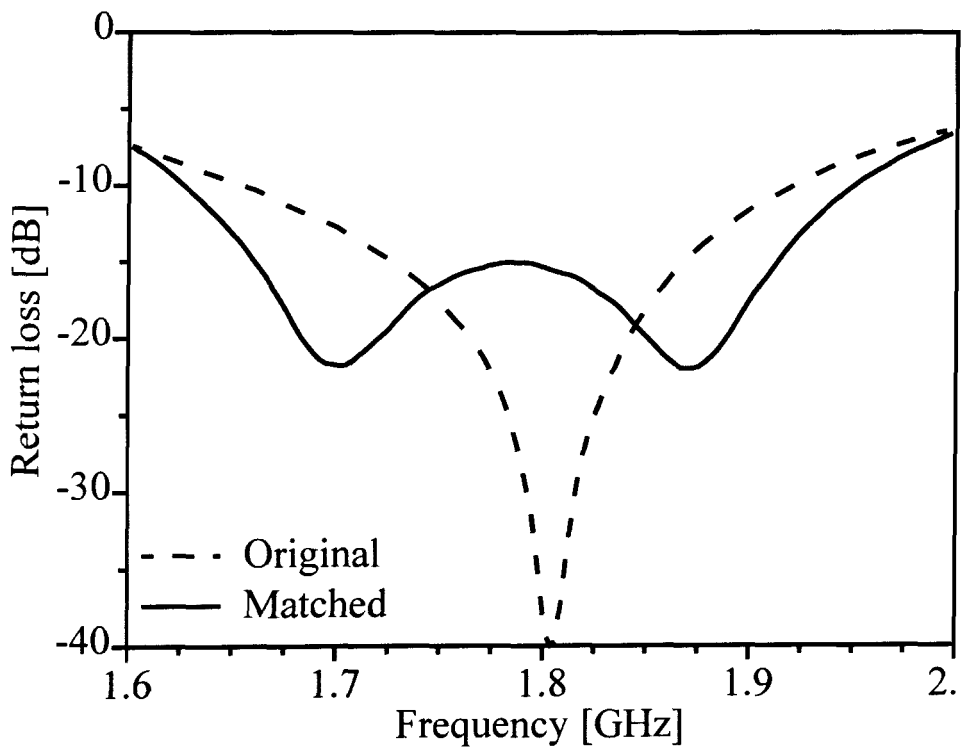

Figure 5.27 Measured return loss for the 10 mm air patch antenna

In the three examples presented in the last three sections, it was proven that the technique for impedance bandwidth improvement works very effectively. One conclusion that does, however, stand out is the fact that it seems as if the SRMT-circuit tends to work less effectively as the patches become more wideband. The percentage improvement obtained for the patches differs from the best improvement for the "substrate-only" patch (164%), to 80% for the 10 mm air patch antenna example. A possible explanation for this is shown in Figure 5.28. The phase transformed imaginary admittance of all three patch antennas is presented in Figure 5.28. The curves are all scaled relative to their VSWR 1.5:1 bandwidth.

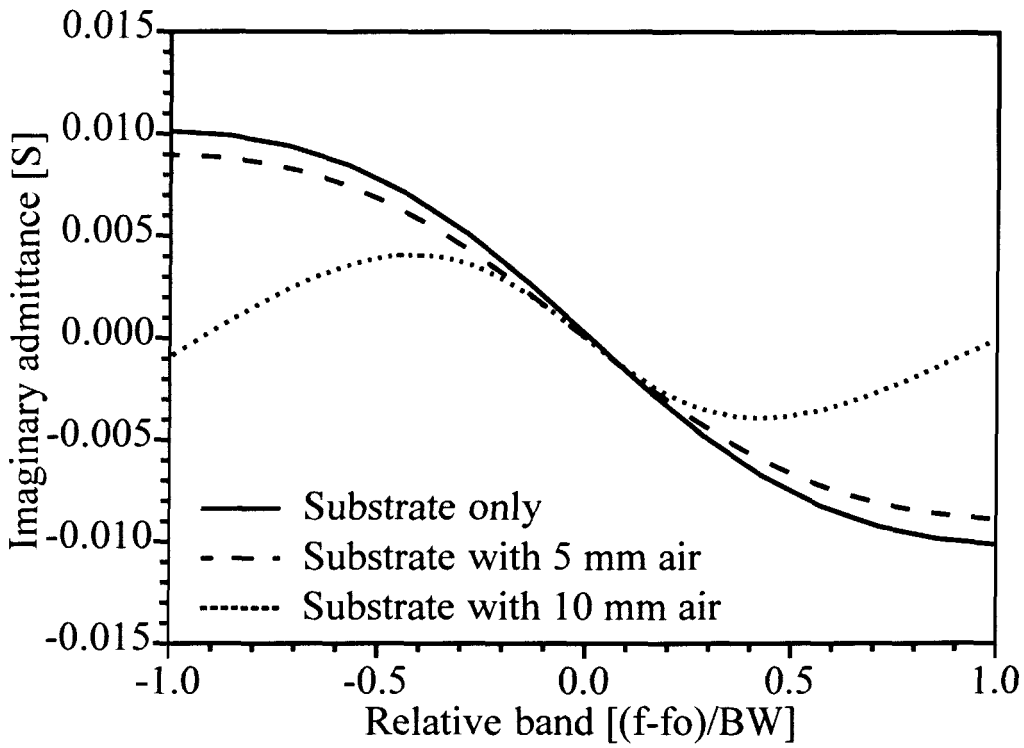

Figure 5.28 Bandwidth scaled version of the phase transformed imaginary admittance for the different patch antennas

In Figure 5.28 the maximum values of the imaginary admittance are of interest. The "substrate-only" patch antenna reaches a maximum value of ±0.01 S. The 5 mm air spaced patch antenna has a maximum of 0.009 S, and the 10 mm air substrate patch antenna only 0.004 S. The main purpose of the SRMT-matching network is to reduce the imaginary admittance for better antenna bandwidth. The "substrate-only" patch antenna has a relatively large reactive component in its input impedance very close to the resonant

frequency. Reducing the reactive component will then inevitably have a substantial effect on the overall performance. That is why the SRMT-circuit is very effective for this type of antenna. On the other hand, the 10 mm air patch antenna has a much-reduced reactive component in its input impedance. Therefore removing this reactive part will not yield the same improvement as in the case of the "substrate-only" patch antenna.

5.4 Coupled lines matching circuit performance compared to the SRMT

In Chapter 2 a matching circuit that implements a coupled line structure is shown [18]. This technique is similar to the coupled lines used for antenna arrays first discussed in [17]. The equivalent circuit of the quarterwave coupling section is a parallel LC-circuit in conjunction with a series transformer [21]. This resonant behaviour, which is present in both the quarterwave coupling structure and the SRMT, shows that the basic principles of both circuits are similar. In [18] it is illustrated how the VSWR bandwidth of an edge-fed patch antenna is increased by adding a quarterwave coupling line to the feed circuit whilst simultaneously feeding the patch antenna with another coupling section (Figure 2.8). The published result of the patch when fed normally and with the edge-fed coupled line is shown in Figure 5.29.

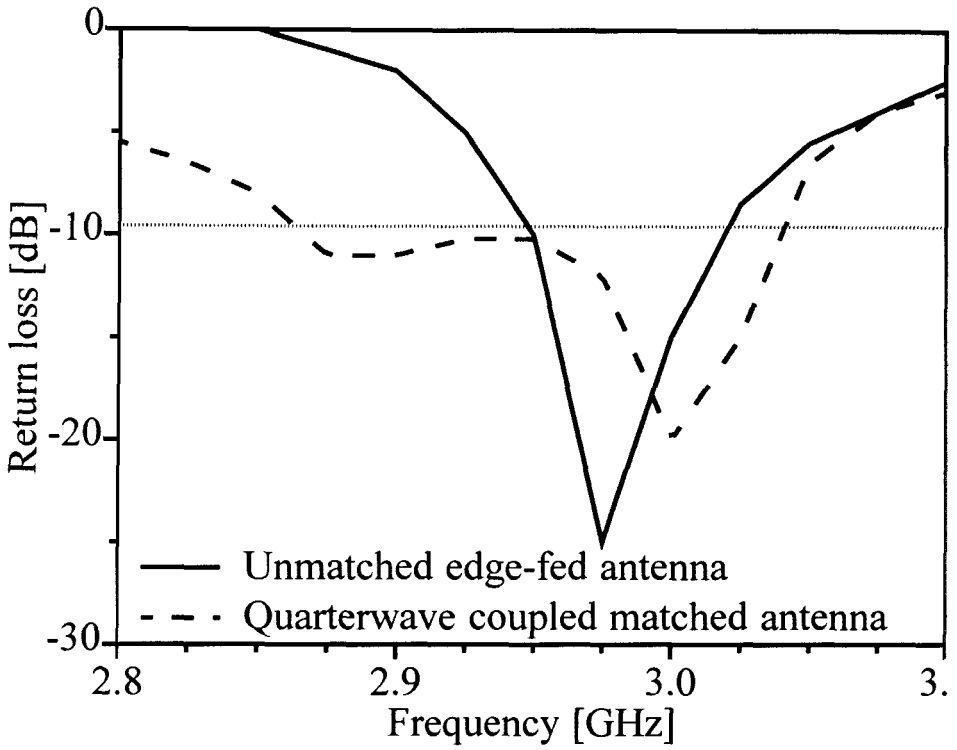

Figure 5.29 Return loss published in [18] for the edge-fed patch and the quaterwave coupled feed line implemented on the patch

The data shown in Figure 5.29 is taken from [18], but only discrete values every 25 MHz are reproduced. The data is not perfectly accurate, but the frequency range below a VSWR of 2:1 is still represented accurately in Figure 5.29. The design frequency of the patch antenna is 3 GHz, and the effective bandwidth obtained for the patch antenna is in the order of 65 MHz. The antenna with the quarterwave coupled lines included has a bandwidth of close to 150 MHz. Note that the values are all approximate since they are read from the published graph [18]. The co-pol radiation pattern of the two patch antennas, shown in [18], exhibits slight beam squint with the addition of the feed structure. Both in the E-plane and H-plane a squint in the order of 7° is obtained. No statements are made regarding possible cross-pol degradation.

The input impedance of the edge-fed patch antenna in the publication [18] is matched to 50 Ω with the addition of a quarterwave matching transmission line. This impedance transforming function is incorporated in the design of the quarterwave coupled line

sections. In Figure 2.8 it is evident that there are two quarterwave coupled sections in the feed network. One section couples to the patch antenna, while the second section couples to the feed line. The equivalent circuit mentioned in [18] is somewhat more complex than the SRMT circuit. To evaluate how the additional complexity affects the circuit's performance in comparison to the SRMT circuit, a similar patch antenna was designed and matched. The design frequency used is 3 GHz. The final antenna prototype obtained with IE3D is shown in Figure 5.30.

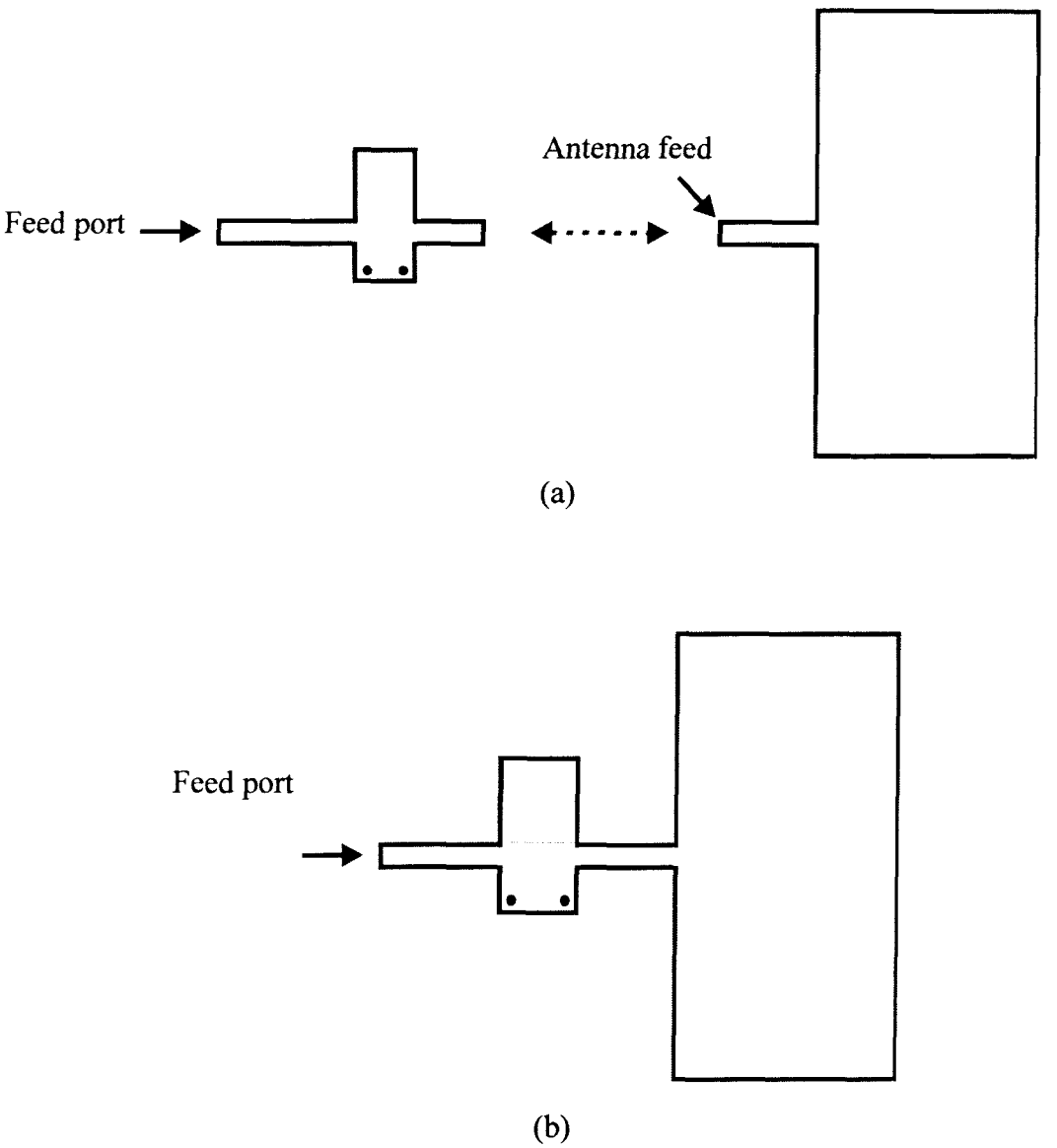

Figure 5.30 Edge-fed patch antenna with matching section. In (a) the matching designed was done separately while (b) has the matching section included as part of the design

Figure 5.30 shows two topologies for the matching of the patch antenna. In all the probe-fed patch antenna examples presented and discussed so far in this chapter, the feed section and the antenna could be separated during simulation because of the intervening ground plane. The edge-fed patch antenna was first designed in a similar fashion, as illustrated in Figure 5.30(a). The patch was considered on its own, and the S-parameters obtained from the simulation were then used for the design and optimising of the LC-resonant section. In principle this would lead to an answer that would show the validity of the matching circuit. It was, however, not the case. The fact that the SRMT-circuit is on the same side of the ground plane as the radiating patch antenna forced the researchers to have the antenna included in the simulation of the matching circuit. This setup is illustrated in Figure 5.30(b). The Smith chart illustration of the results obtained for the SRMT-match is shown in Figure 5.31.

The results for the designed matching circuits for both the separate theoretical design and the combined simulated circuit are presented in Figure 5.31.

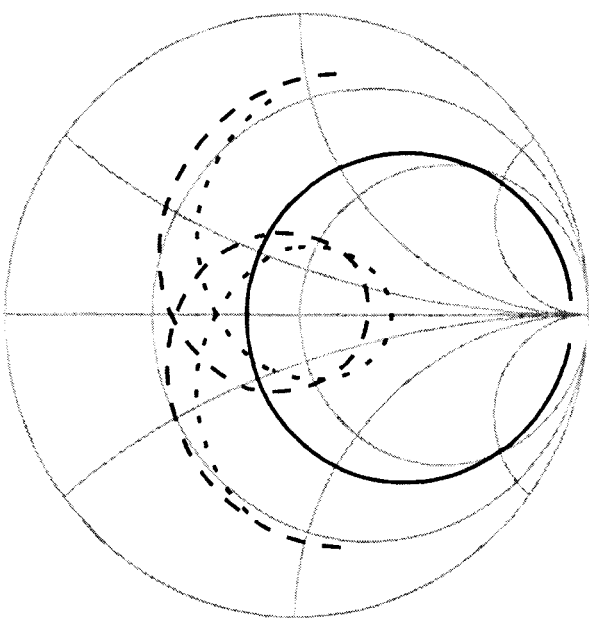

—— Phase transformed unmatched edge-fed

- - - Theoretical SRMT

– – Complete matched

Figure 5.31 Smith chart impedance curves for the edge-fed antenna, shown together with the theoretical circuit design and the combined simulation

The unmatched antenna shown in Figure 5.31 has a resonant frequency input impedance of 83 Ω. The impedance locus shown is already phase-transformed for the SRMT, in order for all the curves on the Smith chart not to lie on top of one another. The unmatched antenna is considered without a quarterwave matching transmission line, since this can be an integral part of the SRMT-design and the antenna already exhibits a VSWR 2:1 bandwidth (Figure 5.32). The first attempt at matching the antenna was made in theory with the raw edge-fed antenna input impedance data. The locus is shown with the dotted line in Figure 5.31 and 5.32. The circuit was created in IE3D for simulation, as shown in Figure 5.30(b). The best response obtained with additional tweaking is shown in Figures 5.31 and 5.32 with the dashed lines.

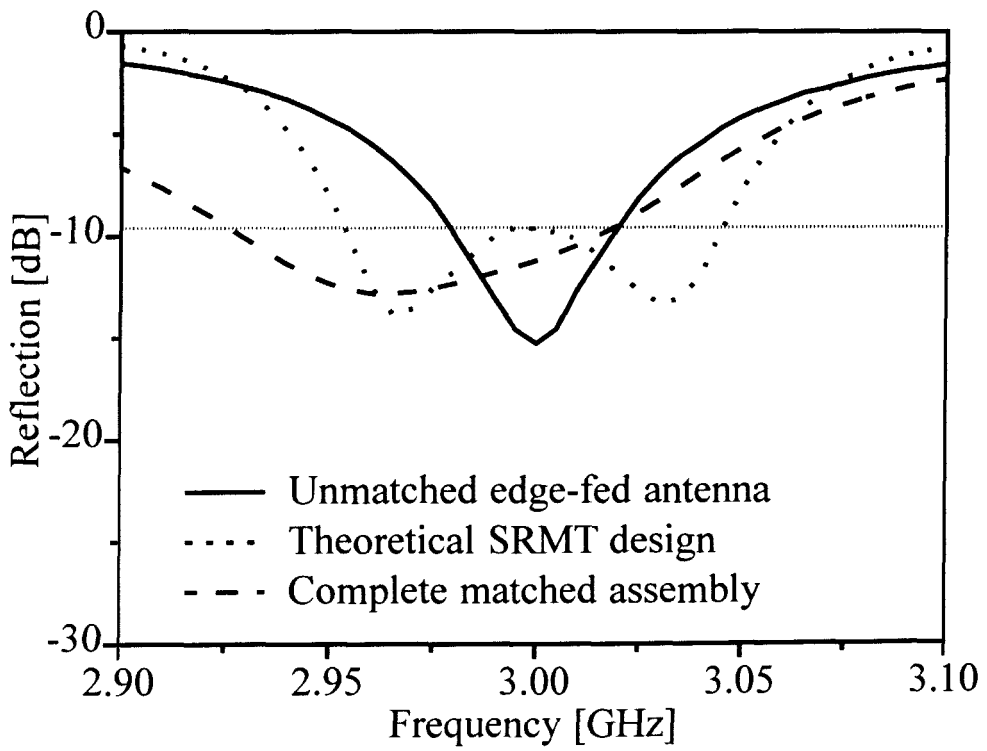

Figure 5.32 Return loss for the edge-fed patch antenna

The unmatched antenna has a VSWR < 2:1 bandwidth of 40 MHz, between 2.98 and 3.02 GHz. The bandwidth increased to 90 MHz with the addition of the theoretically calculated SRMT-match, and the complete simulation also reached a bandwidth of 90 MHz. Although the results for the theoretical design and the full-wave simulation are both 90 MHz, Figures 5.31 and 5.32 show a problem in the response curve. The problem

seemed to be substantial coupling between the patch antenna and the SRMT-circuit. The extra stubs close to the radiating element interfered with the antenna's input parameters and simultaneously the antenna induced currents on the open and shorted stub so that varying the width or length of the stub had little or no effect on the matching of the circuit. The stubs in turn introduced substantial unwanted radiation, as can be seen in the cross-polarisation levels presented in Figure 5.33 and 5.34.

The improvement results are, percentage-wise, very close to the results presented in [18]. The SRMT presented a bandwidth improvement of 125%, from 40 MHz to 90 MHz. The quarterwave match example in [18] improved the edge-fed patch antenna from 65 MHz to 150 MHz, an improvement of 131%. Despite the difficulties encountered in the software implementation of the edge-fed SRMT-match, the result for the circuit is only 6% less in improvement than the published structure. The published structure, on the other hand, is limited in terms of generality, since it is only an option for edge-fed patch antennas. These antennas can only be implemented where no air substrate is considered, thus already limiting the possible bandwidth of the antenna. Secondly the quarterwave-coupled structure has two resonators, since there are two coupled sections. The SRMT aims to match with only one resonant circuit. Space occupancy is also a problem for the quarterwave-coupled structure, as has been explained in [17]. In this section the difficulty in obtaining the resulting match is described, but in [18] only the final result is published. Therefore, it is unknown whether strong coupling between the patch and the matching coupled lines also influenced the results in [18], as was the case with this example.

The simulated radiation pattern of the matched and unmatched edge-fed patch antenna is shown in Figure 5.33 and Figure 5.34. In Figure 5.33 the E-plane pattern is shown. The simulation is presented with an infinite ground plane and no pattern is available from +90° to –90°. The E-plane without the matching circuit has no cross-polarised radiation component. The addition of the matching circuit introduced cross-polarised radiation reaching –20 dB, still acceptably low. The co-pol radiation pattern is changed slightly. The H-plane radiation pattern, presented in Figure 5.34, shows even less radiation distortion in co-pol. The cross-polarisation levels increase from about –34 dB to close to –19 dB. Note that no statements are made regarding cross-polarisation in [18]. In [18] a beam squint is

obtained with the addition of the quarterwave coupled lines. The addition of the SRMT-circuit did not change the co-pol radiation beam squint, and the cross-pol radiation pattern is changed slightly, but the levels still remain well below the co-pol maximum values.

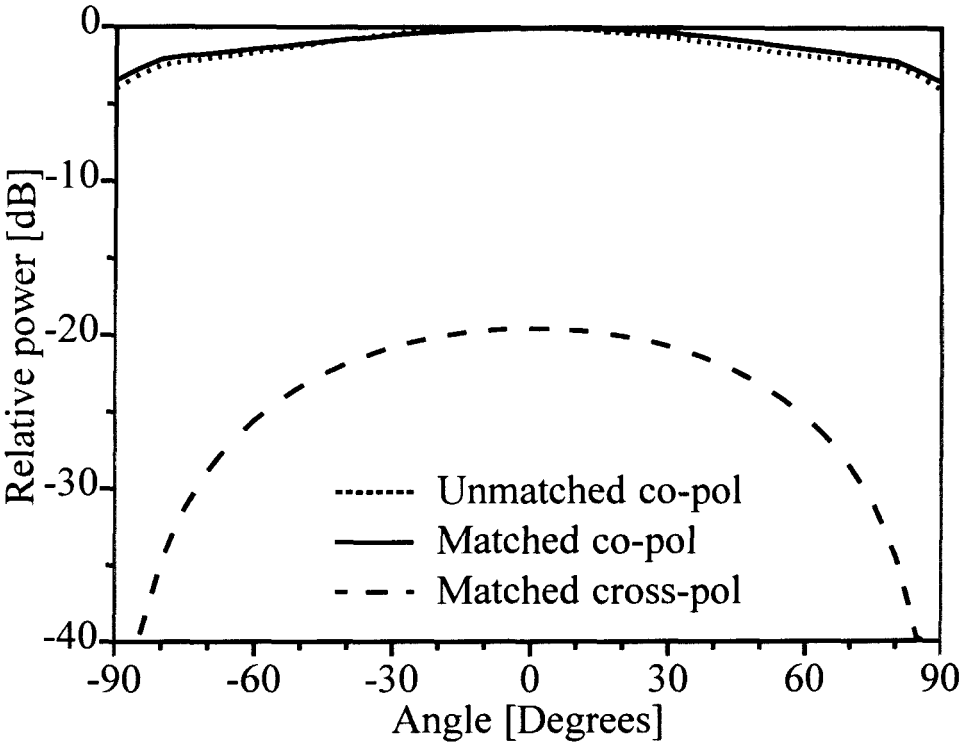

Figure 5.33 E-plane radiation pattern of the edge-fed patch antenna

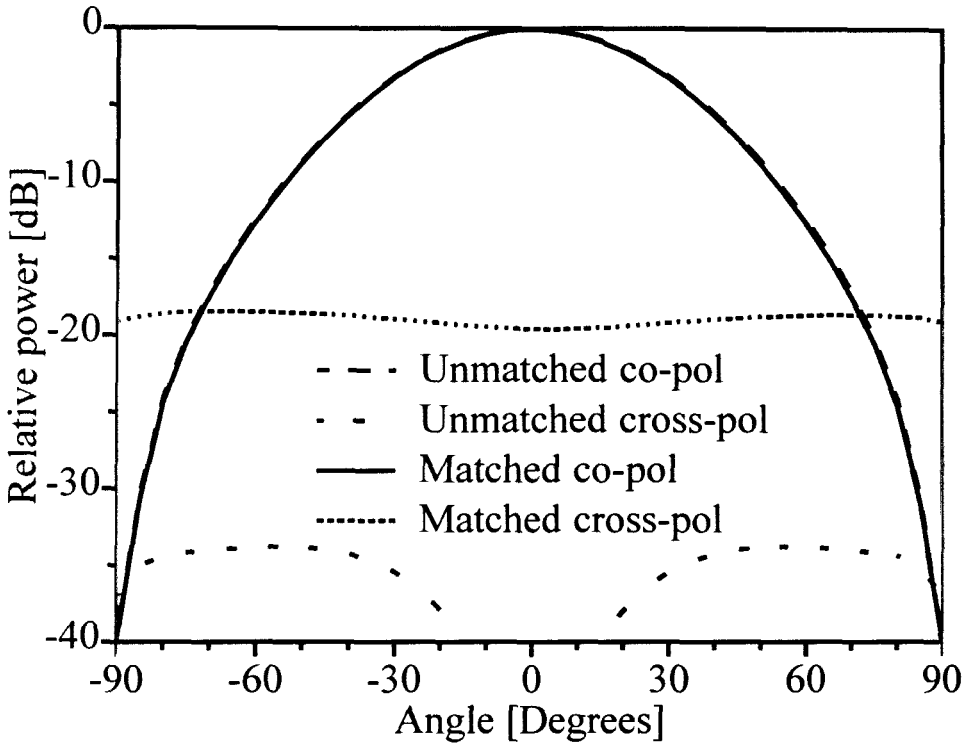

Figure 5.34 H-plane radiation pattern of the edge-fed patch antenna

5.5 Summary of bandwidth enhancement results

In the previous few sections a number of examples were given where the SRMT was implemented on different patch antennas. The results are summarised in Table 5.1. Explanations for the variations were discussed in Section 5.3. Only the edge-fed patch antenna is not verified experimentally, but the main aim with this antenna was to compare the matching circuit in a different setup. It is shown in principle that the SRMT can also work with other types of patch antennas than the probe-fed version.

Table 5.1 Bandwidth operation of the matching network with the patch antenna, expressed in percentage bandwidth and percentage improvement

Antenna	VSWR	Own simulated results			Measured results		
		Original band (%)	Matched band (%)	Improvement factor (%)	Original band (%)	Matched band (%)	Improvement factor (%)
5 mm air	1.5:1	2.78	7.22	160	3.22	6.89	113.8
Substrate only	1.5:1	0.78	1.83	136	0.78	2.06	164
10 mm air	1.5:1	8.67	16.11	85.6	8.83	14.5	64.2
Edge-fed	2:1	1.33	3	125	2.17 [18]	5 [18]	131 [18]